20XX-01-XXXX

On the behavior of the Start & Stop System in European Real Driving Emissions tests and its effect on Greenhouse and Tailpipe Emissions

Teresa Donateo, Piergiorgio Signore

University of Lecce, Department of Engineering for Innovation, Lecce, Italy

Abstract

The Start/Stop system (S/S) is a technology that switches off the engine without the intervention of the driver when the vehicle is stopped. The goal of this device is to eliminate the consumption of fuel associated with the idling of the engine, and consequently, save CO2 and pollutant emissions. However, its effectiveness is related to the percentage of the total driving time with the vehicle stopped. Moreover, even if the S/S is installed and the vehicle is stopped, the S/S can be inhibited by the condition of the vehicle like, for example, a too low state of charge of the battery. This investigation evaluates the actual effect of S/S on tailpipe gaseous emissions in Real Driving Emission tests compliant with the new European Regulations (E-RDE). The investigation is based on data from on-road and on-track RDE tests performed with a Portable Emission Measurement System on a Diesel SUV. From the analysis of these data, the reduction of emission guaranteed by the S/S system was found to be quite lower than the potential in the NEDC test due to the limited activation of the S/S system in real driving tests. Moreover, the analysis put into evidence that the saving associated with the S/S could be counterbalanced by the engine restart especially if the stop time is shorter than a certain threshold.

Introduction

The necessity of reducing the environmental impact of transportation has led in the years to the introduction of more and more stringent emissions standards. Until a few years ago, European emissions regulation used the New European Driving Cycle procedure (NEDC) for the type-approval of vehicles. This procedure suffered from many criticisms, mainly because it was based on laboratory tests that did not reflect the quantity of exhaust emissions emitted during real driving conditions, especially for NO_x emissions [1]. In particular, the NEDC cycle was criticized for its low acceleration pattern, constant speed cruising, and a high number of idling events, which do not represent real-world transient accelerations regimes [2, 3]. From September 2017, the European Commission adopted a new type-approval procedure called WLTP (Worldwide harmonized Light vehicles Test Procedure) [4] that takes into account the class of the vehicle, allows an individual gear shifting pattern for each vehicle, and makes use of driving cycles characterized by realistic speed profile, higher maximum speed, more acceleration, and braking events, shorter stop time, longer driving cycle time and distance.

Through the EU6d Emissions Regulation, the European Commission introduced also Real Driving Emissions (RDE) tests as an additional requirement to the WLTP procedure. The transition towards these new emissions regulations is also connected to the so-called "Dieselgate" scandal that revealed how multiple car manufacturers deliberately exploited "flexibilities" in official emissions testing procedures to manipulate NOx emission data [5]. Diesel vehicles produce less CO_2 per km than gasoline cars of the same class, even in real-world conditions [6], thanks to their highest part low efficiency. This effect is counteracted by the very high values of NO_x in real-world conditions especially when compared with those measured with the NEDC procedure [6,7].

RDE tests are carried out on the road with Portable Emissions Measurements systems (PEMS) and therefore, allow a truer assessment of tailpipe emissions under real-world driving conditions. On the other hand, the results of these tests are deeply affected by the driver behavior, ambient conditions, road profile, and road traffic. The proposed investigation originates from the analysis of on-road and on-track RDE Tests compliant with the new type-approval procedure that were performed on a diesel light-duty diesel vehicle [8,9]. One of the causes of irreproducibility and non-repeatability pointed out in that previous works was the high randomness in the activation of the Start/Stop system that the authors decided to address in the present investigation.

The Start/Stop system is a technology designed to reduce CO_2 emissions and to save fuel by switching off the engine without the intervention of the driver when the vehicle is stopped. In this way, the fuel quantity burned in idling is saved. When the driver shows the intention to drive, the engine is restarted automatically [10]. Many authors in the literature classify star/stop systems as a form of hybridization called Micro HEVs characterized by a degree of hybridization of less than 5%, even if the vehicle is propelled only by the ICE [11-13]. In 2008 only 5% of new cars were equipped with Start/Stop system in Europe [13-14] but the number has increased rapidly over the years so that in 2017 many different car manufacturers implemented the Start/Stop system and almost 100% of the vehicles produced by German car manufacturers were equipped with this system [15]. Since its first introduction, the Start/Stop system was subjected to several developments to obtain a smoother and faster engine restart and better NVH (Noise, Vibration, Harshness) quality. In comparison with conventional vehicles, the battery used for Start/Stop must be able to start the engine a high number of times and to sustain limited or extended engine-off periods [16]. Therefore, new kinds of Lead-acid batteries based on AGM (Absorbent Glass Mat) technology, have been studied [17] for this application. Nevertheless, the literature on S/S systems is quite limited. Some of the works are focused on the reduction of noise and vibration during the engine restart (see for example reference [10] where a Pneumatic Start-Stop system is proposed) or to guarantee a faster restart [18-21]. Other works on the Start/Stop system address technological issues like the application of automatic transmissions with torque converter [22], or the mechanical connection between the electric machine and the engine [23-24].

The improvement in fuel economy (and consequently in CO_2 emissions) that can be achieved by using the S/S system strongly depends on the specific driving cycle. In a standard chassis dynamometer NEDC test, the use of the Start/Stop system and regenerative braking was proved to guarantee a 5.3% improvement of fuel economy in the city cycle and about 4.0% improvement in the extra-urban part [24]. Similar results are reported in [25, 26] where NEDC is compared with WLTC, and the estimated improvement on CO_2 emissions in the WLTC is found to be significantly less relevant due to the shorter idling period. The effect of driving cycle specification on the fuel consumption with S/S technology for a spark-ignition engine is also pointed out in [27]. The benefit of S/S is found to be maximum for the NYCC cycle (3.7 stops per kilometer, 31.0% of idling time) and null for the HWFET one (0,1 stop per km with 1.5% of idling time). However, these results were obtained by numerical simulation assuming that the Start and Stop is activated any time when the vehicle is stopped. In the experimental investigation of [28], it was found that the start and stop system shut off the engine about 53% of the total vehicle stopped time in real driving tests performed with a gasoline start and stop the vehicle. This could be caused by the relatively cold engine oil temperature and the low battery state of charge. In fact, Dimaratos et al. [26] addressed, qualitative, the effect of the extra load on the engine during the restart when the battery was discharged and the consequent increase of fuel consumption and CO_2 emissions and suggested that this effect could counterbalance the benefit from S/S especially in cases of short stop times. However, this discussion was again only qualitative and related to spark engine as in the case of [29]. Santos et al [30] pointed out the negative effect of the S/S on engine durability due to the interruption of oil circulation and consequent reduction of the fluid film over the components when the engine is turned off. None of the above-cited works refers to Diesel engines and none of them quantifies the actual effect of Start & Stop on a real driving emission test compliant with the new European regulation.

To the authors' knowledge, the only interesting work on the emissions of diesel vehicles performing RDE tests is the investigation of Franco et al. [31]. From their results, only 1.33% of the cumulative NO_x emissions in the whole cycle are associated with the engine idling. However, this work does not specify if the vehicle is equipped with the S/S system. Since these issues are not sufficiently addressed in the literature, in particular under RDE tests, the authors propose and apply a methodology for quantifying the actual usage of the S/S system in such tests. The procedure quantifies the emissions associated with the different phases of the driving cycle (traction, braking, coasting, stop with the engine on and stop with engine off) and performs a comparison between actual and potential saving of emissions with the S/S system, which is the novel contribution with respect to the state of the art. Moreover, this work puts into evidence the importance of analyzing the additional emissions caused by the engine restart after the shutting off.

Experimental setup and E-RDE tests

The experimental data used for the investigation are related to a class 3b vehicle (maximum speed >120 km/h, power-to-unladed-mass ratio > 34 W/kg) whose specifications cannot be reported because of a confidentiality agreement. The vehicle was type-approved in 2013 and had a mileage of 70000 km when the tests began. The powertrain includes a Diesel engine and an 8-gears automatic transmission. The after-treatment system consists of a Diesel Particulate Filter (DPF) and a Selective Catalytic Reduction (SCR) system.

For the investigation, the vehicle was endowed with an AVL PEMS 493 as shown in Figure 1. This unit includes multiple gas analyzers, a GPS receiver (to record vehicle speed, latitude, longitude, and altitude), an exhaust flow meter, an exhaust temperature sensor, and an interface for connection to the vehicle's On-Board Diagnostics (OBD). Unfortunately, most of the signals from the OBD, for example the fuel flow rate, the catalyst temperature, and the actual EGR values were not recorded (signals equal to 0 all over the tests).

Note that the emissions of particulate were not measured because the research project was mainly aimed at analyzing the trade-off between CO_2 and NO_x. Ambient temperature, humidity, and pressure were measured using appropriate sensors, but the vehicle was not equipped with catalytic converter temperature sensors, so this information was not available. The accuracies of the measurement devices included in the PEMS are reported in Table 1. All quantities are obtained with a sampling frequency of 10Hz.

Figure 1. The vehicle equipped with the PEMS instrumentations

Note that the presence of the Diesel particulate filter introduces a further disturbing effect on the results of the methodology and causes an increase in CO_2 emissions. However, using the data on exhaust temperature, it was possible to detect the start of regeneration and verify that this does not affect the results of the investigation as explained later.

Table 1. Accuracy of the AVL PEMS

	Range	*Display Resolution*	*Accuracy*
CO	Linearized range: 0 … 49999 ppm Display range: 0 … 15 vol%	1 ppm	0 … 1499 ppm: ± 30 ppm abs 1500 … 49999 ppm: ± 2% rel.
CO_2	0 … 20 vol%	0.01 vol%	0 … 9.99 vol%: ±0.06 vol% abs 10 … 20 vol%: ±2% rel.
NO	0 … 5000 ppm	0.1 ppm	±0.2% FS or ± 2% rel.
NO_2	0 … 2500 ppm	0.1 ppm	±0.2% FS or ± 2% rel.
THC	0 … 30000 ppmC1	0.1 ppmC1	±5 ppmC1 or ± 2% rel.

The new European type-approval procedure is developed in four legislative packages [32]; the most relevant for this investigation are the Commission Regulation (EU) 2016/427 (RDE Act 1) and the Commission Regulation (EU) 2016/646 (RDE Act 2). These two actions define the tests procedures and the boundary conditions. The

tests performed in this investigation will be denoted henceforth with the acronym E-RDE to distinguish them from general tests performed under real-world conditions [33,34] not compliant with the strict requirements of the RDE legislation.

Nine E-RDE tests were performed with the same vehicle and the same driver on-road and on-track. The on-track tests were performed to reduce the effect of ambient conditions, road profile, and road traffic on the emissions of the vehicle [9].

It is important to underline that the goal of this investigation was to analyze the actual behavior of the start and stop in RDE tests compliant with the new type-approval procedure. For this reason, the activation of the Start and Stop was deliberately not controlled (but only monitored) during the E-RDE Tests.

On-road tests

The four on-road E-RDE tests (each with a duration between 93 and 108 minutes) were performed in Lecce, Italy, along the route of Figure 2 on different days with the same driver and the same vehicle configuration (Table 2).

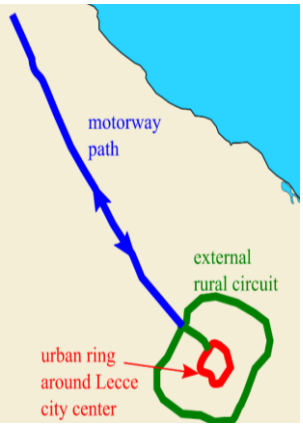

Figure 2. The route used for the urban, rural, and motorway sections of the RDE tests

Table 2. Boundary conditions for the test on the vehicle

	Setting	*Notes*
Payload	12.2% of vehicle weight	Instrumentation, driver, and passenger
Fuel tank	Fully loaded	
Fuel quality	Diesel B7	Same for all tests
Tire pressure	Manufacturer's recommended values	Checked before every test
Headlamps	OFF	Front LED daytime lights ON
Gear shift mode	Automatic	8-gears automatic transmission
Start & stop	Activated	

Table 3 summarizes the specification of the four tests that were performed on-road from 2017/06/09 to 2017/09/07 at the rush time (between 10:30 a.m. and 1:15 pm). Data were sampled with a frequency of 10 Hz. In particular, the average speed of the vehicle in each section is reported for each test in the first row of Table 3. Note the large variability of the average speed in the urban section due to the different traffic conditions that also affect the duration of the whole test (second row) ranging from 93 to 108 minutes. The average urban speed is almost inversely proportional to the number of samples with positive accelerations (third row) that is a measure of the test dynamicity. In the on-road tests, the average temperature varied from test to test between 29.2°C and 38 °C while relative humidity ranged from 25% to 45% (see Figure 3) with limited variation during each cycle as underlined by the standard deviations that are shown in the figure as error bars.

Table 3. Specifications of the E-RDE tests

			Test R1	*Test R2*	*Test R3*	*Test R4*
Variable	*Unit*	*Section*				
Average speed	km/h	Urban Rural Motorway	26.4 72.2 101	21.9 74.4 102.5	23.8 75.4 107.3	19 75.2 100.9
Time	Min	Urban Rural Motorway Total	58 22 13 93	67 20 12 99	62 20 12 94	76 22 10 108
N° of samples with positive accelerations N_k	#	Urban Rural Motorway	1258 370 211	1412 320 194	1302 357 192	1538 365 175
Adherence to Commission Regulation 2016/427			NO	YES	YES	YES

Note that Test R1 is not a real E-RDE test, because the driver did not reach the speed of 110 km/h as required by the Regulation EU 2016/427 for the motorway section.

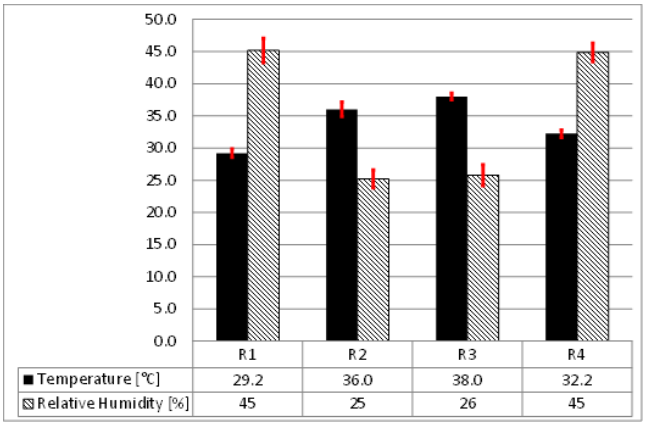

Figure 3. Average values and standard deviation (error bar) of temperature and relative humidity during the tests on-road.

Figure 4 compares the time histories of speed and the speed/acceleration diagrams of one of the E-RDE cycles performed on the route of Figure 2 with the NEDC and the WLTP Class 3b cycles. The NEDC cycle consists of four repeated ECE-15 urban driving cycles (UDC) and one Extra-Urban driving cycle (EUDC), while the WLTP cycle consists of four phases (low, medium, high and extra-high speed). Compared to NEDC, the WLTP class 3 cycle is more realistic. It covers a wider range of engine conditions and is more representative of real driving. It has higher speeds (the maximum and average speed with stops are 131.3 km/h and 46.5

km/h, respectively), steeper accelerations, and decelerations. In the E-RDE test, however, the vehicle acceleration covers an even wider range of operation conditions, and the cycle is much longer. In particular, the E-RDE cycle has higher decelerations at lower speeds and higher deceleration and accelerations at high speeds compared to the WLTC; the former condition occurs when the driver slows down before proceeding at intersections or stops, the latter when overtaking another vehicle. Note also that decelerations are much steeper, mostly in the urban path. However, these features depend on the vehicle category, the driving style, and the traffic conditions [35-37].

Compared with NEDC, the stop time of the vehicle expressed as a percentage of the total driving time), is very low for the WLTC and E-RDE tests as shown in Table 4. Among the E-RDE tests, the vehicle stop time was found to be the highest in test R4 (15.2%) and the lowest on test R3 (where is about a third of the NEDC datum).

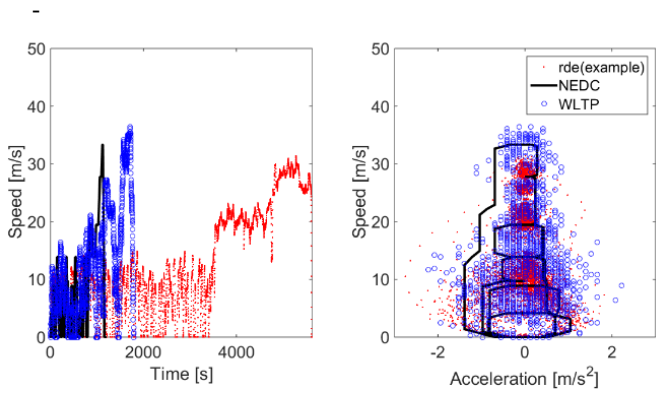

Figure 4. An example of the E-RDE cycle measured on the route of Figure 2 compared with the NEDC and WLTP laboratory cycles

Table 4. Percentage of time spent with the vehicle stopped in each test

		Test R1	*Test R2*	*Test R3*	*Test R4*	*NEDC*	*WLTC*
Variable	*Unit*						
Total trip time	s	5570	5956	5653	6504	1180	1808
Stop time	%	10.4	12.3	8.8	15.2	24.5	12.9

The differences among the four tests generate not only a different stop time but also a different usage of the start & stop system. When the vehicle is stopped, the engine is turned off only if some enable conditions are satisfied. In particular, the S/S is activated only after checking that there are no related faults of the Start/Stop system and the request of automatic stop function is not inhibited [14]. This happens when:

- The state of charge of the battery (SOC) is too low;
- The engine hood is opened;
- The driver is not on the seat;
- The brake vacuum is not sufficient;
- The air-condition is running;
- There are engine sensors error;
- The catalyst temperature is not suitable;
- The cooling water temperature is too high or too low.
- Trigger conditions of engine automatic stop include:
- Current vehicle speed is below 5 km/h;
- Accelerator pedal is released completely;
- Gear is in a neutral position.

On-track tests

The on-track tests were carried out on the circular track of the Nardò Technical Center (NTC) that is 12.5 km long and consists of four lanes for cars and motorcycles and a separate inner ring for trucks. Note that Commission Regulation (EU) 2016/427 requires the vehicles to be tested with PEMS on public roads and to respect local road traffic legislation and safety requirements. Therefore, these on-track tests, are not valid for the homologation process. The regulatory cycles NEDC and WLTC were also reproduced on track. The tests were performed from 2017/07/18 to 2017/09/08.

To reproduce the target speed profile, an in-house interface was developed for the driver and implemented in a laptop mounted on board the vehicle. During the test, the driver visualized both the speed profile of the target cycle and the actual speed value that the GPS is sending to the computer at a given second of acquisition. Two simulated LED lights were added to help the driver follow the speed profile. The route repeatability on a test track was found to be acceptable as regards the reproduction of the speed profile as shown in Figure 5. For more details, refer to [9].

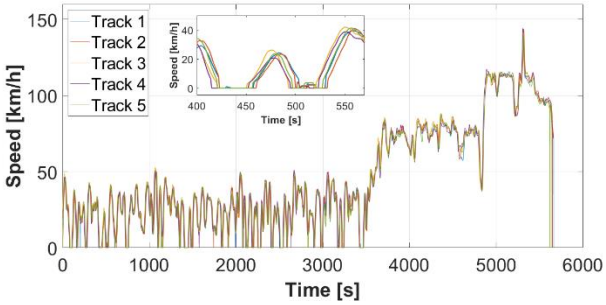

Figure 5. Superimposing the speed profiles in tests T1-T5

Five track reproductions of test R3, named T1-T5, were carried out with the same boundary conditions of Table 2 except for the headlamps that were always turned on (due to track security standards) and the air-conditioning that was activated in tests T1, T2, and T3.

The elevation profiles of the road and the track are shown in Figure 6. The route profile is almost constant in the urban section and ranges from 30 to 60m above sea level. The presence of the valley (0m) and the peak (80m) around 4600s is due to an overpass in the external circle of the route. The track shows a slightly higher driving severity (the maximum altitude is 80 m). Its profile is cyclic versus distance (but not versus time) because the circular lane was traveled about six times to reproduce test R3. Shifting from the urban to the motorway section, the vehicle speed increases, which reduces the duration of the peak in the final part of the track altitude profile versus time. Despite their differences, in both cases (track and route) the altitude was found to be always lower than 100m. Therefore, the effect on engine load is expected to be negligible.

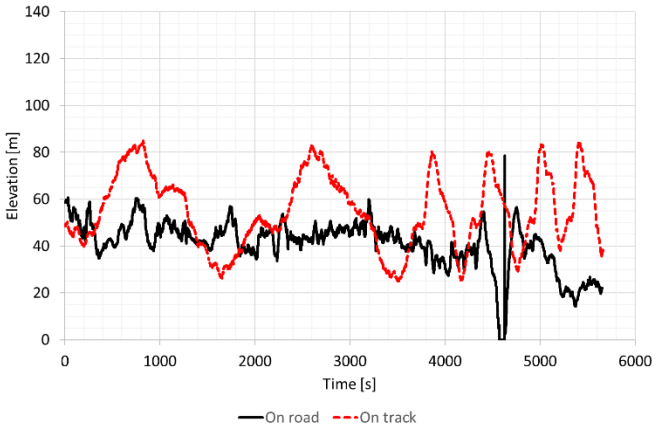

Figure 6.Elevation profile of testing track vs city route

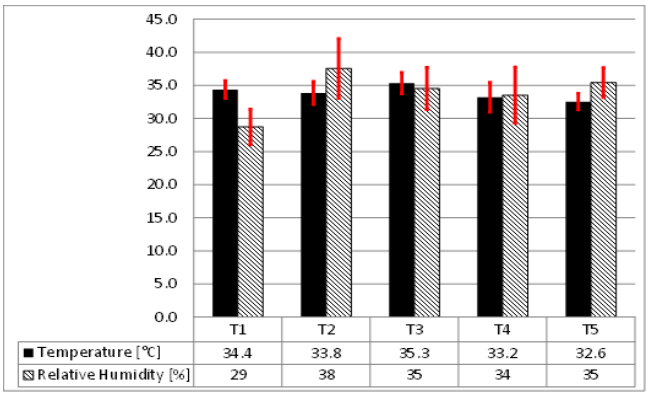

Figure 7. Average values and standard deviation (error bars) of temperature and relative humidity during the tests on the track.

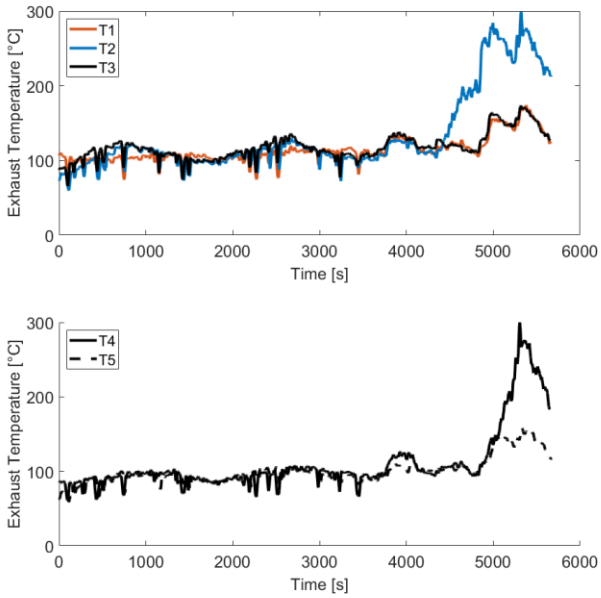

Figure 8. Tailpipe gas temperature measured by the PEMS during the on-track tests

The on-track tests were also performed in summer under hot conditions. The average levels of temperature and humidity are shown in Figure 7 together with the standard deviations of the same variables shown as bar errors. With respect to the tests on-road, the average values of temperature and humidity are less variable from test to test.

During the tests on the track, the regeneration of the particulate filters took place in the rural section for test T2 and in the motorway section for test T4. The regeneration can be spotted by the sudden increase of the exhaust gas temperature as shown in Figure 8. The regeneration caused an increase in the overall emissions of CO_2 in these tests. However, this does not influence the discussion carried out in this work because the S/S system is used only in urban conditions.

The procedure

The tests on-track and on-road described in the previous section are used in the present investigation to quantify the actual contribution of S&S on the overall emissions of a diesel vehicle performing an E-RDE cycle. The following procedure was developed and applied for this analysis:

1. Identification of the driving mode (traction, braking, coasting, and stop, with and without S/S enabled);
2. Analysis of stop time and usage of S/S in E-RDE tests;
3. Quantification of the Actual Saved Emissions (ASE);
4. Quantification of the Potential Saved Emissions (PSE);

The amount of mechanical energy required by a vehicle to follow a pre-fixed driving pattern depends on three main effects [38]: the aerodynamic friction losses, the rolling friction losses, and the energy dissipated in the brakes. The elementary equation that describes the longitudinal dynamics of a road vehicle can be written as:

$$m_v \frac{d}{dt} v(t) = F_t(t) - (F_a(t) + F_r(t) + F_g(t) + F_d(t)) \quad (1)$$

Where

- F_a is the aerodynamic force;
- F_r is the rolling friction;
- F_g is the horizontal component of the gravitational force (for roads with slope);
- F_d is the disturbance force that summarizes all other not yet specified effects. These effects are not considered in the following discussion, because they are not directly related to vehicle dynamics;
- F_t is the traction force, that is the force generated by the prime mover minus the force that is used to accelerate the rotating parts inside the vehicle and minus all friction losses in the powertrain;
- m_v is the vehicle mass. This is equal to the sum of the "curb weight" (defined by the vehicle manufacturer) and a payload (e.g. weight of the driver and passengers, luggage, etc.);
- $v(t)$ is the instantaneous speed of the vehicle and the term $m_v \frac{d}{dt} v(t)$ represents the inertial force.

After assuming appropriate values for the rolling and drag coefficient from the literature [11], the authors used the values of speed and elevation (Figure 6) acquired by the GPS to calculate the traction

force and to identify the driving phases of the vehicle at any time in the driving cycle:

- if $F_t(t) > 0$, the vehicle is assumed in traction phase;
- if $F_t(t) < 0$, the vehicle is braking;
- if $F_t(t) = 0$ and $v(t) = 0$, the vehicle is in stop phase;
- if $F_t(t) = 0$ and $v(t) > 0$, the vehicle is in coasting.

The position of the acceleration pedal obtained from the OBD was used to verify the results. When the vehicle is stopped, the data acquired from the OBD scanner are used also to distinguish, according to the values of the engine rpm, the stop phases with the engine turned off (S/S on) or with the engine idling (S/S off).

The PEMS measures the concentration of the emissions (expressed in ppm for NO_x, CO, HC, and vol% for CO_2) and the exhaust gas flow in liter/h, the exhaust gas temperature in °C, and the pressure in kPa. Based on these signals, the flow rate in g/s of each gas was calculated in this investigation with the following equation [39]:

$$\dot{m}_{gas}(i) = u_{gas}(i) \cdot c_{gas}(i) \cdot \dot{m}_{mew}(i) \qquad (2)$$

where:

- $\dot{m}_{gas}$: mass flow rate of the exhaust component *i* [g/s];
- u_{gas}: ratio between the density of the exhaust component *i* to the overall density of the exhaust, as listed in Table 5;
- c_{gas} measured concentration of the exhaust component "i" in the exhaust [ppm];
- $\dot{m}_{mew}$: measured exhaust mass flow rate, converted in kg/s;

Since the gas flow rate is calculated with a mathematical operation from quantities affected by uncertainty (Table 1), the authors applied the error propagation theory [40] to obtain an error band for each emission. This is done by referring to the accuracy of the data obtained from the PEMS (see (eq. (2)) and that of exhaust gas flow, temperature, and pressure as defined by the technical standard [39,41] (Table 6).

Table 5. Density ratio of each exhaust gas in a Diesel engine. Data were taken from Ref. [39]

Fuel	ρ_e [kg/m^3]	u_{gas}			
		NO_x	CO	HC	CO_2
Diesel (B7)	1.2943	0.001586	0.000966	0.000482	0.001517

Table 6. Accuracy of the measurement parameters.

Measurement parameter	***Accuracy***
Exhaust gas flow	±2% of reading
Temperature ≤ 600 K	±2K (absolute value)
Temperature > 600 K	±0.4% of reading (K)
Pressure	±0.2kPa (absolute value)

The total saving of emissions guaranteed by the S/S system during the total stop time $t_{Stop,tot}$ is evaluated in the following way. First of all, we separated, in each cycle, the total stop time with the deactivated S/S $t_{Stop,off}$ (engine idling) and the stop time with the S/S on (engine turned off), $t_{Stop,on}$ (see Figure 9).

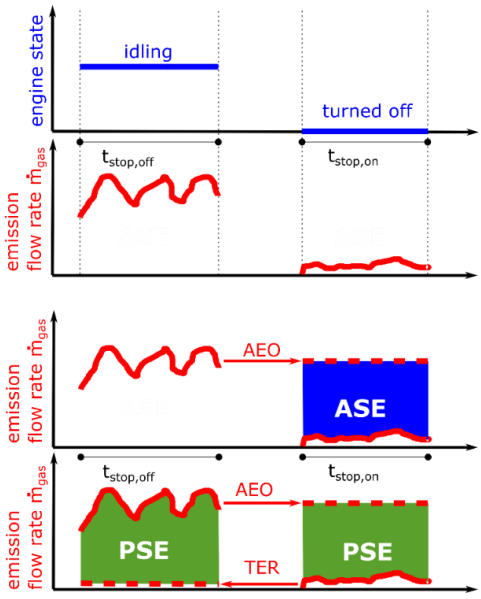

Figure 9. Graphical explanation of the procedure used to evaluate the saved emissions during the stop phases

The average flow rate of each gas in $t_{Stop,off}$ (AEO) is:

$$AEO(i) = \frac{\int_0^{t_{stop,off}} \dot{m}_{gas}(i) \cdot dt}{t_{Stop,off}} \qquad (3)$$

Even if the engine is turned off during $t_{Stop,on}$, the PEMS could measure a certain amount of each gas during this time window. This is due to the delay in the response of the PEMS. When the engine is turned off, theoretically the tailpipe emissions should be zero. In practice, it is necessary to consider the time taken from the exhaust gas to reach the tailpipe as pointed out by Zhang et al [29], and the inertia of the exhaust gases.

The Actual Saved Emissions can be estimated as:

$$ASE(i) = \left[\mathrm{AEO}(i) \cdot t_{Stop,on} - \int_0^{t_{stop,on}} \dot{m}_{gas}(i) \cdot dt\right] \qquad (4)$$

The meaning of ASE is graphically explained in Figure 9. If the S/S is never active in a cycle, then ASE=0. Note that it was not possible to perform tests with the start/stop system always inactive, so we introduced this metric to estimate how much the S/S system had reduced the emissions.

If the S/S would have been always active, the average measured flow rate of gas *i* during $t_{Stop,off}$ would be the average of the same quantity in $t_{Stop,off}$ that we will call TER (threshold emission rate):

$$TER(i) = \frac{\int_0^{t_{stop,on}} \dot{m}_{gas}(i) \cdot dt}{t_{Stop,on}} \qquad (5)$$

Therefore, we can calculate the potential saved emissions of the S/S system by assuming that it is always on when the vehicle is stopped:

$$PSE(i) = ASE(i) + \int_0^{t_{Stop,off}} \dot{m}_{gas}(i) \cdot dt + -TER(i) \cdot t_{Stop,off} \quad (6)$$

This metric is explained graphically in Figure 9. Note that if the S/S is always active during vehicle stops, then ASE=PSE. Therefore, by comparing ASE with PSE one can quantify how well the S&S system has worked in each E-RDE. As for ASE, this metric was introduced because it was not possible to perform tests with the start/stop system always active. Moreover, due to the intrinsic non-reproducibility of the E-RDE tests, it would not be accurate to compare the emissions in the three cases (monitored S/S, deactivated S/S, and S/S always active) measured on three separate repetitions of the test.

Discussion of the results

The proposed procedure was applied to the data acquired on the test case vehicle. The first expected result was that the impact of the phases of stops on the overall emissions is quite negligible because the main contribution to the total emissions is obtained in the traction mode as shown in the plots of Figure 10. The data reported in this vehicle refers to test T1 but similar results are obtained in all the E-RDE cases. Overall, the emissions in the stop phases account only for 0.43% of the total CO_2 emissions on the cycle, 0.88% for NO_x, 0.8% for CO and HC. These results prove that the overall effect of the S/S in a whole RDE compliant with the New European Legislation is completely negligible since most of the emissions are produced when the vehicle is in traction or braking (as also found in [31]). Even if the tests T1-T5 are repetitions of the same cycle, there are some disturbing effects like the variability of ambient temperature and humidity that are expected to be more relevant than S/S usage on the cumulative emissions. The emissions associated with the Stop phases are low for two reasons: the reduced time spent with the vehicle stopped (Table 4) and the activation of the S/S system.

The plot of Figure 11 shows, for all the tests considered in this investigation, the percentage of stop time with the S/S on and off. In the on-track reproduction of tests R3, the total vehicle stop time is almost the same in all repetitions (average value 467.4s, standard deviation 21.7s) but the usage of the S/S strongly differs. In Track 4, 73% of the total stop time is performed with the engine off (S/S on), while this percentage is the lowest for Track 5 (42%). Track 1 and 2 show a similar usage of the S/S system. Remember that tests T1-T5 are repetitions of the same cycle so they differ only for the boundary conditions. These differences show that in real driving conditions, the emissions saving is strongly affected by the state of the battery and the other checks that control the activation of the S/S system.

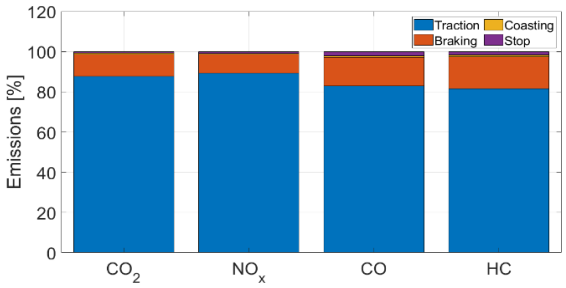

Figure 10. CO_2 emissions in the different driving phases for RDE test "Track 1" with the actual usage of the S/S (measured values)

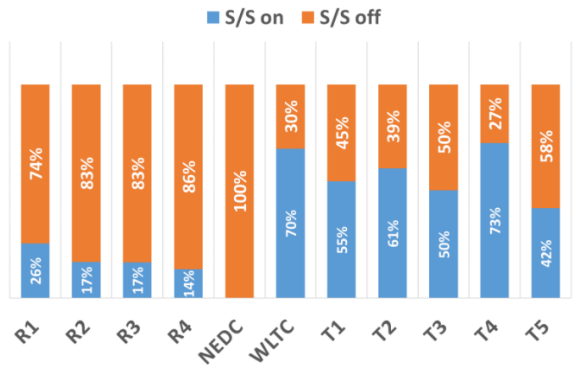

Figure 11. Usage of start & stop in the different tests

Of particular interest are the emissions detected in the E-RDE test "T4", where the Start/Stop system has been active more often than in other E-RDE tests, and the advantages, in terms of cumulative CO_2 and NO_x emissions, are visible (see Figure 12 and Figure 13 where only the emissions in the stop phases are reported). To better quantify the effect of S/S, the authors applied to all tests the metrics PSE and ASE illustrated in Figure 9 and explained in EQs. (4) and (6). The saved emissions are expressed in Figure 14 as a percentage of the emissions measured on the whole test. The results for the on-tracks repetition are shown as average value plus an error bar.

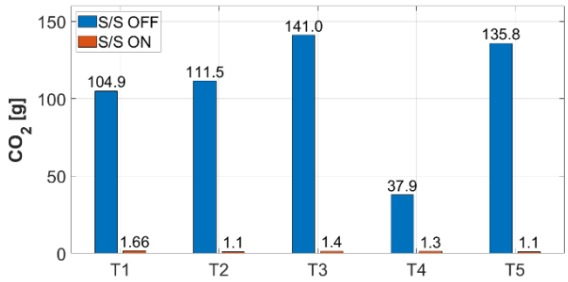

Figure 12. Cumulative CO_2 emissions in the vehicle stop phases, with Start and Stop system ON or S/S OFF.

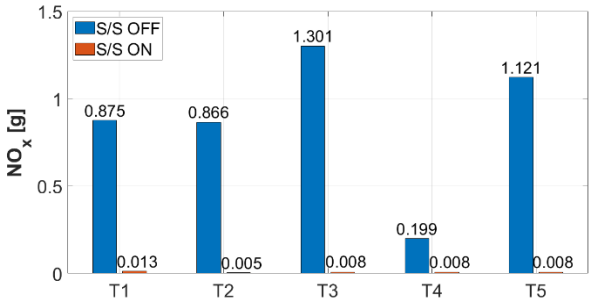

Figure 13 Cumulative NO_x emissions in the vehicle stop phases, with S/S on and off.

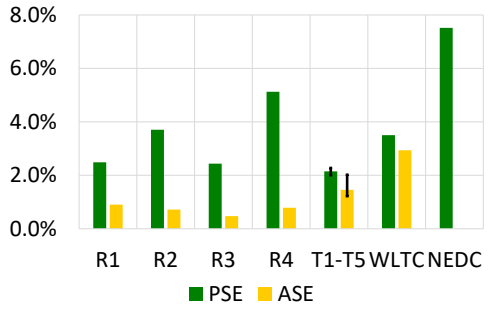

Figure 14. Potential and actual saved emissions of CO_2 guaranteed by the S/S system

Note that the actual saving of CO_2 emissions in the whole E-RDE tests is very low compared with the potential 7.5% estimated in this case for the NEDC cycles. This happens for two reasons. The first one is that the stop time in E-RDE tests is, in percentage, very limited with respect to the NEDC cycle. The second one is that the S/S is only partially exploited (as can be seen in the difference between the potential and actual fuel saving as a consequence of the data in Figure 11). It is possible to notice that the PSE is directly proportional to the percentage of stop time (see Figure 15) while the ASE is affected by the already mentioned factors that inhibit the activation of the S/S.

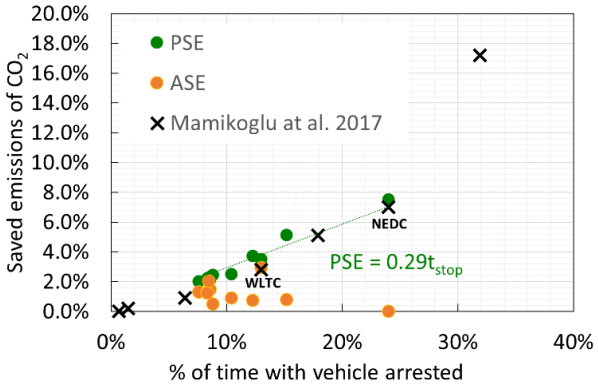

Figure 15. Correlation between saved emissions of CO_2 and percentage of time with the vehicle stopped for all cycles. Data from [27] are reported for comparison and validation

For comparison, the figure also shows the PSE estimated by Mamikoglu et al [27] and in particular, the results for the two cycles common to both investigations, i.e. NEDC and WLTC for a class 3 vehicle. Even if they are related to a gasoline engine, the trend of saved CO_2 emissions/fuel vs % of the time with the idling engine is the same in the range considered in this paper (% of the time with vehicle arrested ranging from 8% to 24%). This can be considered as a validation of the proposed procedure for the evaluation of PSE.

Note that the results discussed in this section refer to the whole E-RDE cycles including the urban, the rural and the motorway segments. The usage of the Start/Stop system, however, affects principally the urban part of the cycle. On the other hand, the goal of this investigation is to study the effect of the Start/Stop system on the whole E-RDE procedure, so a separate analysis of the urban segment is not performed here.

Considerations on the engine restart

For a more complete analysis about the tailpipe gas emissions resulting from the use of the Start/Stop system, it is necessary to evaluate the emissions flow rate not only during the stop but also during the following restart of the engine (Go). To this scope, a time window including the phase of stop and the first instants of vehicle restart is considered and named SGTW (Stop and Go Time Windows). An SGTW is the sum of the time at which the engine is turned off (t_{Stop}) and a certain t_{Go} time corresponding to the restart of the engine (see Figure 16). After an analysis of the emissions flow rate during the restart, we decided to assume, empirically, a duration of 45s for the "Go" phase ($t_{Go} = 45s$). In fact, for the analyzed cases, the emissions mass flow rates were noticed to reach the same value about 45s after the engine restart.

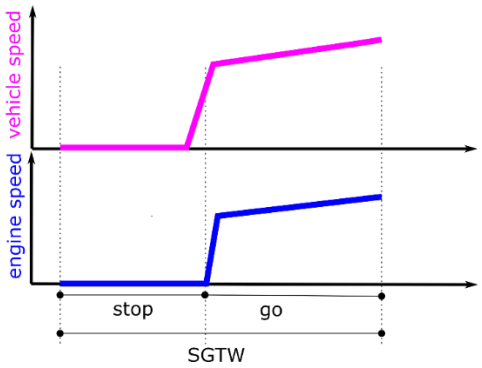

Figure 16. Graphical illustration of the Stop and Go Time Window

Note that the SGTWs are the same for all on-track tests. However, some of them are performed with the engine always on and others with the engine off during the stop, requiring a restart of the engine during the "Go" phase.

The driving cycle reproduced in the on-track tests T1-T5, has a total of 35 SGTWs. However, only two of them were performed in tests T1 and T2 with a different usage of the S/S. They are denoted as SGTW1 and SGTW2 in Figure 17. In both cases the S/S was activated in T2 and "off" in T1. Figure 18 shows the mass flow rates of CO_2, NO_x, HC time with the relative error bands. The vertical dashed lines are the estimated beginning and end of the stop time (t_{Stop}). The emissions of CO were not shown because of their very low value in urban driving conditions. It is well known that the presence of CO in the exhaust of diesel engines assumes a meaningful value only at full load and for engines operating at high speeds [42].

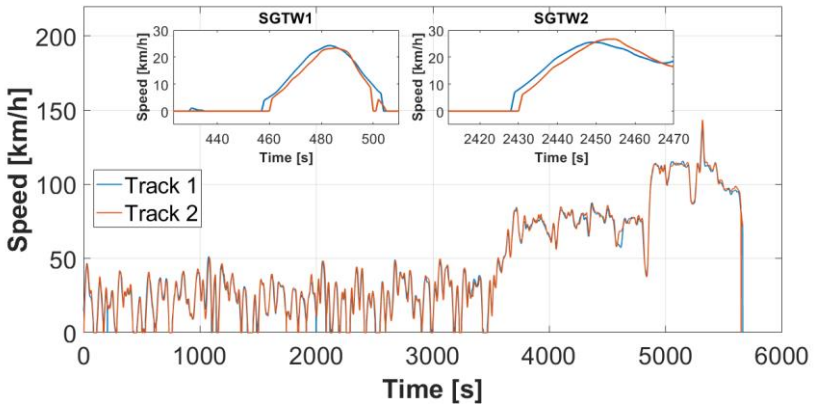

Figure 17. SGTWs considered for the analysis of the emissions during the stop and restart phases.

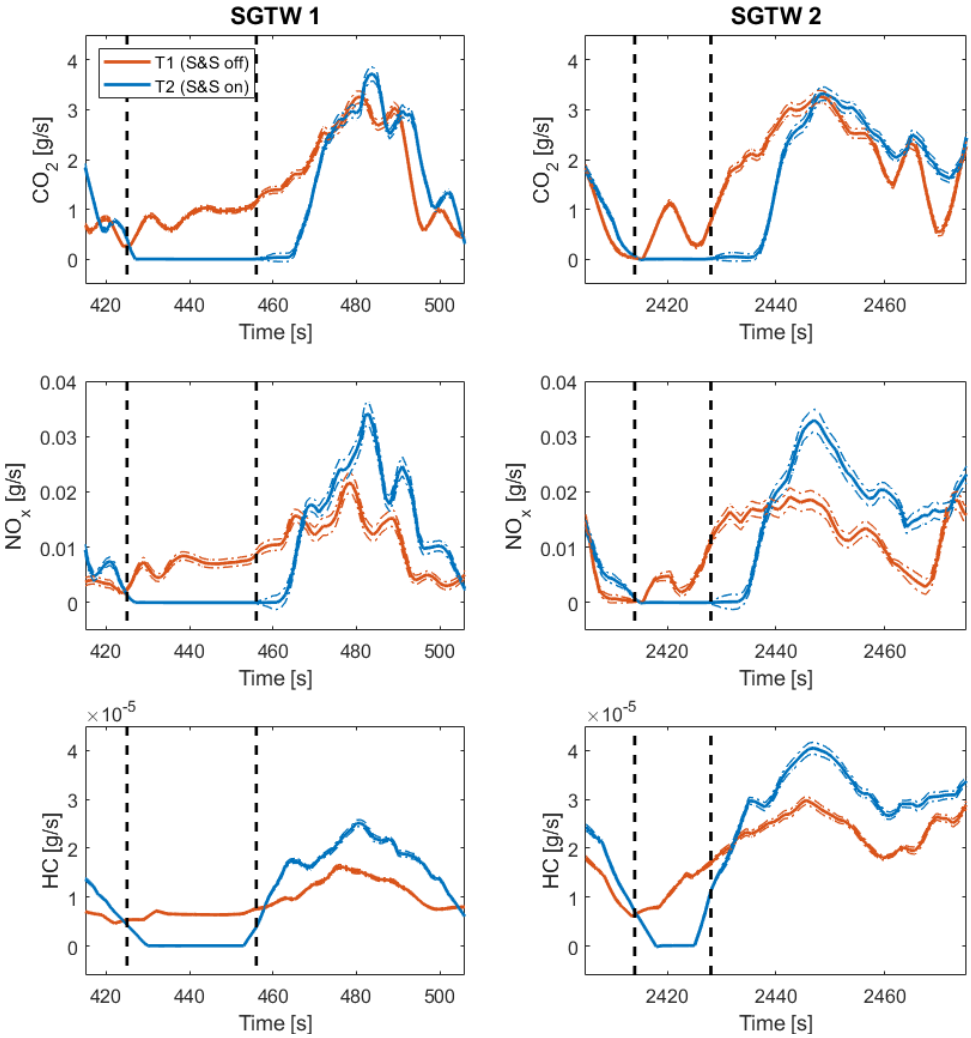

Figure 18. The emission flow rate in SGTW2 for Track 1 (S/S off) and Track 2 (S/S on) with error band. The vertical dashed lines delimit the stop phase.

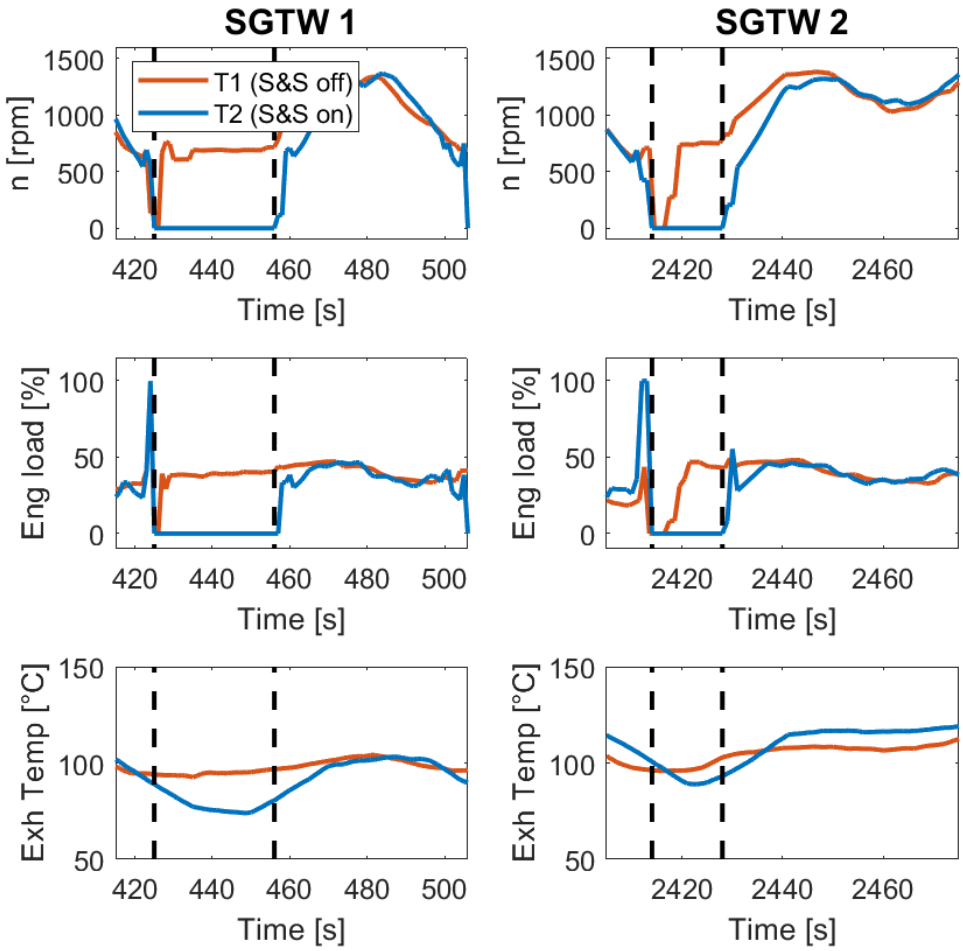

Figure 19. Engine working point and exhaust temperature for Track 1 (S/S off) and Track 2 (S/S on). The vertical dashed lines delimit the stop phase.

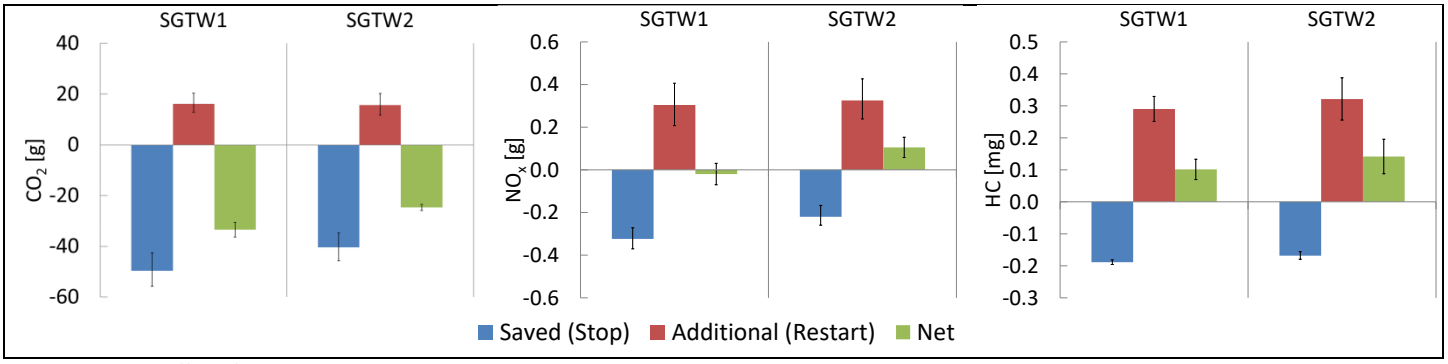

Figure 20. The net effect of S/S in the two SGTW windows

Figure 19 shows the engine speed and load together with the exhaust gas temperature measured by the PEMS. By analyzing this figure, it is possible to note that there is a peak in the engine load and speed at the beginning of restart, particularly in SGTW2 for test T2 (S/S on). In the case of T1, the peak is at the beginning of the stop. This can be explained as pointed out by Dimaratos et al. [26], by the battery recharge that triggers the activation of the alternator that causes, in turn, an extra load on the engine. Note that the conditions of the engine are almost the same in the two cases since we performed repetitions of the same driving test.

The CO_2 mass flow rate in the restart phase (Figure 18) has about the same maximum value with and without the activation of the S/S. Therefore, the restart of the engine does not cause an increase in the

emissions of this gas. The only visible effect of the restart is that the mass flow rate of CO_2 in test T2 (S/S activated) shows a delay with respect to the trend of this component in Track 1 because of the delayed restart of the engine.

As for the NO_x, a very high peak in the mass flow rate is evident during the restart of the engine in the case of S/S on (Track 2) compared with the flow rate obtained during the restart of the vehicle after a stop phase with the engine at idling speed. This behavior can be found also in the HC mass flow rate. Note that the peak of NOx emissions could be better put into evidence by using a high-frequency acquisition system like that used by Zhang et al [29].

The higher pollutant emissions can be explained by the faster increase of load and speed of the engine during the restart from the engine turned off (T2) with respect to the case with the engine idling (T1). As pointed out by Grondin et al. [43] during transients, the intake gas composition and thus the cylinder burned gas ratio are not in steady-state operating conditions leading to spikes in measured NOx. It is also interesting to put into evidence that test T2 was performed on a drier day (in fact, the registered ambient air humidity is lower while the ambient temperature is quite the same as shown in Figure 7). NOx emissions are affected by the intake of air humidity and in particular, the higher the humidity, the lower the NOx emissions [42, 44, 45,46] due to the higher specific heat of the air-fuel mixture. This effect could counteract, in part, the processes described above.

Another possible explanation for the additional emissions during restart could be the interruption of oil circulation and consequent reduction of the fluid film over the components. After starting, until the film is formed again, there may be a more accentuated wear that is known to affect engine durability [30].

A more complete analysis of the reasons behind the emissions behavior should take into account the details of the engine control and the behavior of the aftertreatment systems under transient conditions. Another possible explanation for the additional emissions is that the tailpipe exhaust temperature (see Figure 19) is about 20°C lower in the case with S&S at the restart time. We did not measure the ATS temperature, but we can assume that it is also lower in the case of S/S off when the engine is restarted. Since the efficiency of the SCR is affected by the exhaust gas temperature [44], it is reasonable that the increase of emissions at the restart is caused, at least in part, by the reduced efficiency of the after-treatment system. This analysis, however, is not sufficient to explain the higher emissions of NOx with S/S in the case of SGTW2 where the difference in the exhaust temperature in the two cases, T1 and T2, is less remarkable. One more important phenomenon to analyze is the mixing between the intake gas and the EGR flow and also the possible differences in the control of injection. Unfortunately, the OBD scanner gives no detailed information about this important aspect.

Addressing all these possible aspects is only possible when experiments are performed under controlled conditions because the intrinsic non-reproducibility of RDE tests makes it difficult to understand the exact cause of the additional emission. The goal of the analysis, however, was not to explain but to put into evidence the need of balancing the two effects (the saved emissions when the vehicle is stopped and the additional peaks during restarts).

The SAVED emissions during the stop phase could be calculated as:

$$SAVED(i) = \int_0^{t_{Stop}} (\dot{m}_{gas,off}(i) - \dot{m}_{gas,on}(i))\, dt \quad (7)$$

During the restart the additional emission ADDED(i):

$$ADDED(i) = \int_{t_{Stop}}^{t_{Stop}+t_{Go}} (\dot{m}_{gas,on}(i) - (\dot{m}_{gas,off}(i)) \cdot dt \quad (8)$$

The NET effect of S/S is:

$$NET(i) = ADDED(i) - SAVED(i) \quad (9)$$

According to this definition, the S/S system reduces the emissions of the gas *i* if *NET(i)* is negative. If the NET effect is positive, we can conclude that S/S is ineffective in real world conditions. However, this depends on the duration of the stop phase. So, we could estimate the minimum stop time after which the S/S system determines a reduction of emissions ($min\ t_{Stop}$) by considering the following inequality relation:

$$\mathrm{SAVED(i)} \leq \mathrm{ADDED(i)} \quad (10)$$

In particular, considering the error bands of the signals, the maximum, average, and minimum differences between the signals of each emission are calculated and reported in Figure 20.

According to the results of T1 and T2, the S/S systems guarantee a reduction in CO_2 emissions (and, consequently, in fuel consumption) even considering the restart phase. On the contrary, while there is a reduction in NO_x emissions during the vehicle stop phase, their increase during the engine restart has led to a total increase of NO_x emissions in the SGTW2 while for SGTW1 the balance is quite neutral. As for HC, the usage of S/S increases the emissions of this gas in both windows.

The differences between the two time-windows are also due to the different duration of the stop phase before the restart. In the first time-window, the stop phase lasts 19 seconds, while in the second time-window, it lasts 37 seconds. By applying eq. (8), the authors calculated the minimum stop time to achieve a reduction of emissions with the S/S system. The following results were obtained:

- The estimated time stop needed for zeroing the NO_x emissions is about 37 [s] (which is the stop time of SGTW1);
- The estimated time stop for zeroing the HC is 43seconds.

Note that these results are strictly related to the tests performed in this work and affected by the limited number of data, Nevertheless, they underline the additional emissions associated with the engine restart when the stop phases are too short and the necessity of performing a rigorous experimental campaign to measure the actual effect of S/S in E-RDE tests.

Conclusions

This paper proposes a methodology to quantify the actual saving of emissions guaranteed by an S/S system during a Real Driving Emission test compliant with the European regulation (E-RDE). The procedure was explained by application to a set of experimental data obtained with a Portable Emissions Measurement System on a Diesel SUV by performing 11 driving cycles on road and on track with the same vehicle and the same driver

Due to the intrinsic non-reproducibility of the E-RDE tests, it would not be meaningful to compare the emissions in the three cases (monitored S/S, deactivated S/S, and S/S always active) measured on three separate repetitions of the test. On the contrary, the proposed procedure calculates the actual and potential saving of emissions using the data of the same RDE test.

The application of the procedure put into evidence that, due to the reduced percentage of time spent with the vehicle stopped in an E-RDE test compared with the NEDC, the effect of S/S on the cumulative emissions mass is negligible since most of the emissions are produced when the vehicle is in traction or braking. The potential saving of CO_2 emissions in the eleven tests was found to be directly proportional to the percentage of time spent at zero vehicle speed. However, the actual saving of CO_2 was still lower because the S/S system is not always activated when the vehicle is stopped, i.e. the engine is idling instead of being turned off. Consequently, the Actual Saved Emissions of CO_2 was found to range from 0.5% to 2.9% according to the different specifications of the cycle and to the different usage of the S/S because of the boundary conditions (in particular the state of the battery used to restart the engine).

The analysis of the data revealed a peak of emission when the engine is restarted after the stop, putting into evidence the necessity of considering a time window including the stop and the subsequent restart of the engine for the analysis of the emissions. However, the results of this last part of the investigation are only preliminary and their analysis needs to be addressed with an accurate and complete experimental campaign. Future studies are also needed to address the important topic of cold-start emissions.

Definitions/Abbreviations

AEO – Average Emissions with start and stop deactivated

ASE – Actually saved emissions

BISG – Belt-driven Integrated Starter Generator

EGR – Exhaust Gas Recirculation

EU – European Union

GPS – Global Positioning System

NEDC – New European Driving Cycle

OBD – On-Board Diagnostic

PEMS – Portable Emission Measurement System

PSE – Potential Saved Emissions

E-RDE– Real Driving Emissions Tests compliant with the new European legislation on emissions

RDE – Real Driving Emissions

S/S – Start and Stop

SGTW – Stop and Go Time Window

SCR – Selective Catalytic Reduction

TER –Threshold emissions rate (as measured by PEMS with S/S

WLTC – Worldwide harmonized Light vehicles Test Procedure

References

1. EEA, SAE European Environment Agency, Air Quality in Europe, 2016.
2. EEA, SAE European Environment Agency, Air Quality in Europe, 2015.
3. Varella, R.A., Duarte, G., Baptista, P., Sousa, L. et al., “Comparison of Data Analysis Methods for European Real Driving Emissions Regulation,” SAE Technical Paper 2017-01-0997, 2017, doi:10.4271/2017-01-0997.
4. Ciuffo, B. and Tutuianu, M., “The Development of the World-wide Harmonized Test Procedure for Light Duty Vehicles (WLTP) and the Pathway for Its Implementation into the EU Legislation,” *TRB 2015 Annual Meeting*, 2015.
5. Palmer J., Schwanen T., “Clearing the air after “dieselgate”: Time for European regulations to experiment with participatory governance”, The Geographical Journal, 2019, Volume 185, Issue 2 p. 237-242
6. O’Driscoll R.O., Stettler M.E.J., Molden N., Oxley T., ApSimon H.M., “Real world CO2 and NOx emissions from 149 Euro 5 and 6 diesel, gasoline and hybrid passenger cars”, Science of the Total Environment, Volume 621, 2018, p 282-290.
7. Assanis D.N. – Filipi Z.S – Hagena J.R , "Transient Diesel Emission: Analysis of Engine Operation During a Tip-in", SAE technical paper, 2006, 10.4271/2006-01-1151
8. Donateo, T., Giovinazzi, M., and Tamborrino, A., “Reproducing Real World Emission Tests with a Traffic Simulator,” SAE Technical Paper 2018-37-0001, 2018, doi:10.4271/2018-37-0001.
9. Donateo, T. and Giovinazzi, M., “Some Repeatability and Reproducibility Issues in Real Driving Emission Tests,” SAE Technical Paper 2018-01-5020, 2018, doi:10.4271/2018-01-5020.
10. Gilberti, V., “Pneumatic Start-Stop System,” SAE Technical Papers 2007-01-2767, 2007, doi:10.4271/2007-01-2767.
11. Guzzella and Sciarretta, Vehicle Propulsion Systems, Third Edition, Springer
12. Cardoso D.S., Fael P. O., Erpirito-Santo A. “A review of micro and mild hybrid systems”, Energy Reports Volume 6, Supplement 1, February 2020, Pages 385-390
13. Enang W., Bannister C., “Modeling and control of Hybrid electric vehicles (A comprehensive review), Renewable and Sustainable Energy Reviews 74 (2917), 1210-1239
14. Chen, H., Zuo, C., Yuan, Y., “Control Strategy Research of Engine Smart Start/Stop System for a Micro Car,” SAE Technical Paper 2013-01-0585, 2013, doi:10.4271/2013-01-0585.

15. The international council on clean transportation, “European vehicle market statistics,” Pocketbook, 2018/2019.
16. Kremer, M., Hülshorst, T., “In-market Application of Start-Stop Systems in European,” FEV Inc., 2011, Report No.: P26844-01_01.A1.
17. Lee, S., Cherry, J., Safoutin, M., McDonald, J., “Modeling and Validation of 12V Lead-Acid Battery for Stop-Start Technology,” SAE Technical Paper 2017-01-1211, 2017, doi:10.4271/2017-01-1211.
18. Robinette, D., Powell, M., “Optimizing 12 Volt Start - Stop for Conventional Powertrains,” SAE Technical Paper 2011-01-0699, 2011, doi:10.4271/2011-01-0699.
19. Wellmann, T., Govindswamy, K., Tomazic, D., “Integration of Engine Start/Stop Systems with Emphasis on NVH and Launch Behavior,” SAE Technical Paper 2013-01-1899, 2013, doi:10.4271/2013-01-1899.
20. Wellmann, T., Govindswamy, K., Orzechowski, J., Srinivasan, S., “Influence of Automatic Engine Stop/Start Systems on Vehicle NVH and Launch Performance,” SAE Technical Paper 2015-01-2183, 2015, doi:10.4271/2015-01-2183.
21. Hao, L., Namuduri, C., Gopalakrishnan, S., Lee, C. et al., “Enhancing Engine Starting Performance Using High-Power Density Brushless Starter,” SAE Technical Paper 2020-01-0459, 2020, doi:10.4271/2020-01-0459.
22. Gibson, A., VanDerWege, B., Wooldridge, S., Moilanen, P. et al., “Development of Stop/Start Engine Combustion and Restart Control for Gasoline Direct Injection Automatic Transmission Application,” SAE Technical Paper 2014-01-1747, 2014, doi:10.4271/2014-01-1747.
23. Okuda, K., Komatsu, Y., Nakahara, Y., “Research and Analysis of ISG Belt-drive System for Idling Stop System,” SAE Technical Paper 2006-01-1501, 2006.
24. Bishop, J., Nedungadi, A., Ostrowski, G., Surampudi, B. et al., “An Engine Start/Stop System for Improved Fuel Economy,” SAE Technical Paper 2007-01-1777, 2007, doi:10.4271/2007-01-1777.
25. Beer J., Teulings W., Optimized Start Strategy for Stop/Start Operation of a μ-Hybrid Vehicle, SAE Technical Paper, 2007-01-0298, 2017
26. Dimaratos, A., Tsokolis D., Fontaras G., Tsiakmakis S., Ciuffo B., Samaras Z., “Comparative evaluation of he effect of various technolgoies on light-duty vehicle CO_2 emissions over NEDC and WLTP”, Transportation Research Procedia 14 (2016) 3169 – 3178
27. Mamikoglu, S., Andric, J., and Dahlander, P., "Impact of Conventional and Electrified Powertrains on Fuel Economy in Various Driving Cycles," SAE Technical Paper 2017-01-0903, 2017, doi:10.4271/2017-01-0903.
28. Lee, S., Fulper, C., McDonald, J., and Olechiw, M., “Real-World Emission Modeling and Validations Using PEMS and GPS Vehicle Data,” SAE Technical Paper 2019-01-0757, 2019, doi:10.4271/2019-01-0757.
29. Zhang, Y., Deng, J., Li, Q., Liu, Y. et al., “Characteristics of Transient NOx Emissions of HEV under Real Road Driving,” SAE Technical Paper 2020-01-0380, 2020, doi:10.4271/2020-01-0380.
30. Santos N. D. S. A., Roso V. R., Faria M. T.C. “Review of engine journal bearing tribology in start-stop applications”, Engineering Failure Analysis, Volume 108, 2020.
31. Franco V., Posada Sànchex F., German J., Mock P., “Real-world Exhaust Emissions from Modern Diesel cars”, The international council on Clean Transportation, White Paper, October 2014, retrieved online 15-04-2020.
32. https://ec.europa.eu/growth/sectors/automotive/environment-protection/emissions_en), retrieved April 2020
33. Chen Y., Borken-Kleefeld J., “Real-driving emissions from cars and light commercial vehicles – Results from 13 years remote sensing at Zurich/CH”, Atmospheric Environment, 2014, Volume 88, pp 157-164
34. Pan Y., Chen S., Qiao F., Ukkusuri S.V., Tang K., “Estimation of real-driving emissions for buses fueled with liquefied natural gas based on gradient boosted regression trees”, Science of the total environment, 2019, Volume 660, pp. 741-750.
35. Weiss M, Bonnel P., Hummel R., Provenza A., Manfredi U., “On-Road Emissions of Light-Duty Vehicles in Europe”, *Environmental Science & Technology* 45.19 (2011), pp. 8575–8581.
36. Frey H. C., Unal A. Rouphail N.M., Colar J.D., “On-Road Measurement of Vehicle Tailpipe Emissions Using a Portable Instrument”, *Journal of the Air & Waste Management Association*, 2003, Vol. 53, No. 8, pp. 992-1002, DOI: 10.1080/10473289.2003.10466245.
37. Donateo T., Ingrosso F., Licci F., Laforgia D., “A method to Estimate the Environmental Impact of an Electric City Car during Six Months of Testing in an Italian City”, *Journal of Power Sources*, 2014, Vol. 270, pp. 487-498, doi: 10.1016/j.jpowsour.2014.07.124.
38. Guzzella, L. and Sciarretta, A., Vehicle Propulsion Systems:Introduction to Modeling and Optimization (Berlin: Springer, 2007).
39. Ministry of Land, Infrastructure, Transport and Tourism Announcement, “Attachment 119 to the Announcement that Prescribes Details of Safety Regulations for Road Vehicles,” Technical Standard for on-road exhaust emissions of diesel-powered light-and-medium duty motor vehicles, No. 619, July 2002.
40. "Propagation of Uncertainty through Mathematical Operations" (PDF). p. 5. Retrieved 2020-04-04.
41. Commission Regulation (EU) 2016/427.
42. Heywood, J.B., Internal Combustion Engines Fundamentals (McGraw-Hill, 1988).
43. Grondin O., Thibault L., Quèrel C., “Transient Torque Control of a Diesel Hybrid Powertrain for NOx limitation”, 2012 Workshop on Engine and Powertrain Control, Simulation and Modeling, France, October 23-25, 2012
44. Boriboosomsin K, Durbin T., Scora G., Johson K, et al, “Real-world exhaust temperature profiles of on-road heavy-duty diesel vehicles equipped with selective catalytic reduction”, Science of The Total Environment, Volume 634, 1 September 2018, Pages 909-921
45. Ishida, M., Chen, Z. , 1994, “An Analysis of the Added Water Effect on NO Formation in D.I. Diesel Engines”, SAE Paper 941691;
46. A. de Risi, T. Donateo, D. Laforgia, “Theoretical Investigation on the Influence of Physical Parameters on Soot and NOx Engine Emissions”, **ASME-ICE**-Vol. 36-2, 2001, ISSN**:** 10665048, pp. 53-64